2010 International Conference on Electrical Machines and Systems

October 10-13, 2010, Songdo Convensia, Incheon, Korea

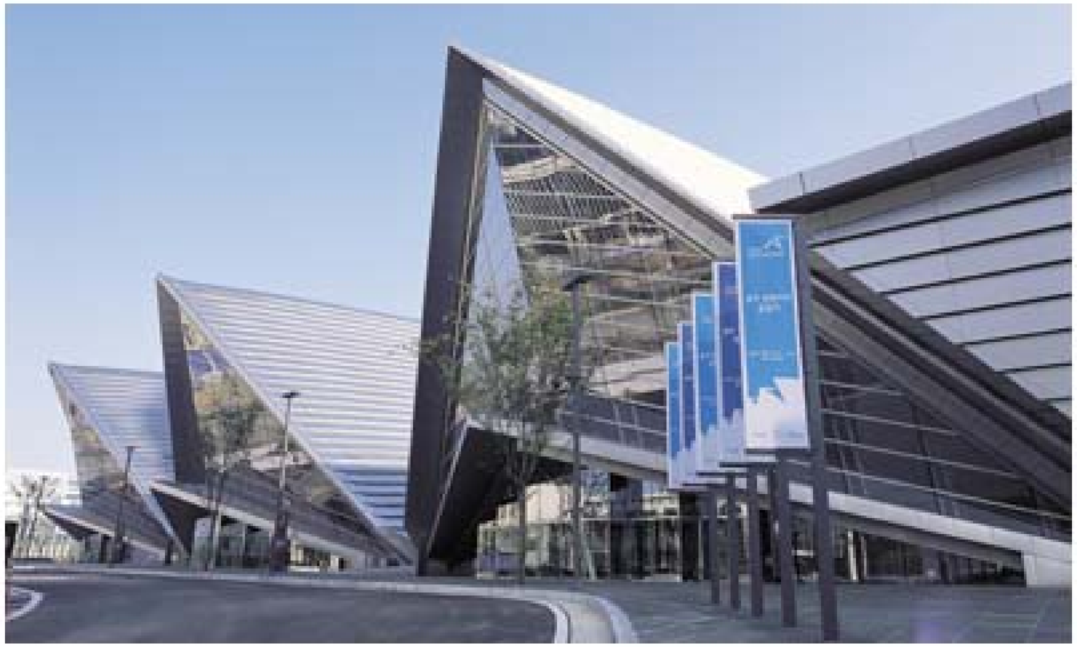

IEEE Catalog Number: CFP10801-CDR
ISBN: 978-89-86510-12-6

Vendor: Prof. Jin Hur
Tel: +82-52-259-1282 / Fax: +82-52-259-1686
E-mail: jinhur@ulsan.ac.kr

Organized by

KIEE (The Korean Institute of Electrical Engineers)

Co-organized by

CES (China Electrotechnical Society)

IEEJ (The Institute of Electrical Engineers of Japan)

Technical Co-sponsor

IEEE Industry Application Society

Jung-Pyo Hong

- The Effect of Silicon Steel Sheet on Core Loss in Induction Motor

Jung-Pyo Hong

- Effect of Vibration and Noise on IPMSM Type Integrated Starter and Generator According to Number of Slots

Jung-Pyo Hong

- Reduction Design of Eddy Current Loss in IPMSM using Response Surface Methodology

Jung-Pyo Hong

- A Study on the Relation Between Rotor Rib and Maximum Power of IPMSM in Flux Weakening Region

Jung-Pyo Hong

- Design of an Interior Permanent Magnet Synchronous In-Wheel for Electric Vehicles

Jung-Pyo Hong

- Vibration Analysis according to Stator Shape Design in a PMSM

Jung-Pyo Hong

- Characteristic Analysis of the Water Pump Motor considering Polar Anisotropic Ferrite Bonded Magnet

Jung-Pyo Hong

- A Study on the Reduction of Noise and Vibration of SPM According to Reduction of Permanent Magnet

Jung-Pyo Hong

- Evaluation and Improved Design about Acoustic Noise and Vibration in IPMSM

Jung-Pyo Hong

- Reduction Eddy Current Loss Design and Analysis of In-Wheel Type Vehicle Traction Motor

A Study on The Relation Between Rotor Rib and Maximum Power of IPMSM in Flux Weakening Region

Ho-Kyoung Lim, Baik-Kee Song, Sung-Il Kim, Jung-Pyo Hong
Dept. of Automotive Engineering, Hanyang University, Korea
E-mail: hongjp@hanyang.ac.kr

Abstract — This paper investigates the change of maximum power of an Interior Permanent Magnet Synchronous Motor (IPMSM) according to the rotor rib without the alteration of design factors related to the motor. As increasing the thickness of a rotor rib, it relieves stress concentration when the rotor rotates at high speed. However, the amount of leakage flux which comes from the PM makes the performance reduction of IPMSM. On the contrary, as a rib thickness is reduced, the opposite pattern occurs. Therefore, a decision of the rotor rib thickness is important. In addition, a rib thickness affects the d, q axis inductances and these factors result in the variation of the output power of IPMSM in the flux weakening region. Especially, as d-axis inductance changes, higher torque can be obtained. As a result, by redesigning the rotor rib, maximum power increased by ten percent in some cases. Therefore, the relation between rotor rib and maximum power of IPMSM in flux weakening region is identified by using finite element analysis (FEM) and equivalent circuit analysis.

I. INTRODUCTION

Lately, the high efficient electric motors have been demanded in many industrial filed. The Interior Permanent Magnet Synchronous Motor(IPMSM) is used widely because both magnetic torque and reluctance torque can be used simultaneously. Due to possibility of flux weakening operation through current vector control, IPMSM is suitable for the motor that demands high power density and high efficiency [1].

In the flux weakening region, if the voltage ellipse moves to the left, the power density increases at the same angular velocity. In order to move the voltage ellipse, a characteristic current should be changed. There are two kinds of alternatives for this purpose. First of all, increasing no-load linkage flux is one of the methods by using more permanent magnet(PM). However, EMF increases linearly in proportion to the angular velocity of rotor and then EMF reaches the limit which is IGBT breakdown voltage. Also, PM occupies a large portion of the price of the motor. Secondly, by reducing d-axis inductance, the voltage ellipse is shifted to the left. In other words, the characteristic current moves to the left side, then the voltage ellipse will cross the upper constant torque locus. Thus, the power density rises.

In this paper, for enhancing the power density in flux weakening region, the rib design considered thickness without additional PM is suggested.

II. CALCULATION OF VOLTAGE ELLIPSE IN IPMSM

The IPMSM is commonly analyzed using two axis theory. The *d*-axis is defined in the direction of the rotor permanent magnet flux linkage phasor so that the orthogonal *q*-axis is aligned in with the open circuit EMF phasor [2]. The equivalent circuits for IPMSM based on a synchronous reference frame including iron losses are presented in Fig. 1. The mathematical model of the equivalent circuit is given in the following equations. The *d, q*-axis voltages and currents are given by (1), (2), and (3).

$$V_a = \sqrt{v_d^{\,2} + v_q^{\,2}}\ ,\ I_a = \sqrt{i_d^{\,2} + i_q^{\,2}} \tag{1}$$

$$\begin{bmatrix} v_d \\ v_q \end{bmatrix} = R_a \begin{bmatrix} i_{od} \\ i_{oq} \end{bmatrix} + \left(1 + \frac{R_a}{R_c}\right) \begin{bmatrix} v_{od} \\ v_{oq} \end{bmatrix} + p \begin{bmatrix} L_d & 0 \\ 0 & L_q \end{bmatrix} \begin{bmatrix} i_{od} \\ i_{oq} \end{bmatrix} \tag{2}$$

$$\begin{bmatrix} v_{od} \\ v_{oq} \end{bmatrix} = \begin{bmatrix} 0 & -\omega L_q \\ \omega L_d & 0 \end{bmatrix} \begin{bmatrix} i_{od} \\ i_{oq} \end{bmatrix} + \begin{bmatrix} 0 \\ \omega \psi_a \end{bmatrix} \tag{3}$$

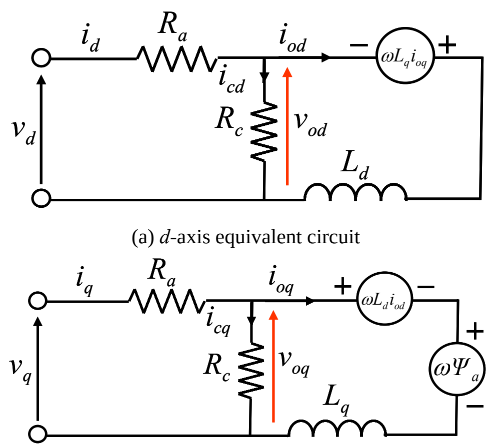

(a) *d*-axis equivalent circuit

(b) *q*-axis equivalent circuit

Fig. 1. Equivalent circuit of the IPMSM model in the *d*-*q* reference frame

where, i_d and i_q are the *d, q*-axis component of the armature current, i_{cd} and i_{cq} are the *d, q*-axis component of iron loss current, v_d and v_q are the *d, q*-axis component of terminal voltage, R_a is the armature winding resistance per phase, R_c is the iron-loss resistance, Ψ_a is the flux linkage of PM per phase root mean square (rms), L_d and L_q are *d, q*-axis inductance.

The equations (2-1), (3-1) can be obtained by applying the assumptions that the state is steady and the terms of resistive voltage drop are small at high speeds in equations (2), (3).

$$v_d = -\omega L_q i_{oq} \tag{2-1}$$

$$v_q = \omega (L_d i_{od} + \psi_a) \tag{3-1}$$

When the equations (2-1), (3-1) are applied at equation (1), the voltage ellipse equation is obtained like (4).

$$\left(\frac{i_d + \frac{\psi_a}{L_d}}{\frac{\psi_o}{L_d}}\right)^2 + \left(\frac{i_q}{\frac{\psi_o}{L_q}}\right)^2 = 1 \quad (4)$$

III. Shift of the Center of Voltage Ellipse

The voltage ellipse and current circle trajectories from inverter and motor establish operating limits of the drive system. The control strategy must select these commands that satisfy both trajectories [3].

The center of voltage ellipse is called a characteristic current that is the ratio of No-load linkage flux to the d-axis inductance. The characteristic current I_{ch} is given by (5).

$$I_{ch} = -\frac{\psi_a}{L_d} \quad (5)$$

When the characteristic current is placed within current circle, it is possible to use the field weakening control. Fig. 2 is shows voltage ellipses and constant torque loci. If the characteristic current is shifted from A to B, the voltage ellipse will cross the upper constant torque locus. Finally, the maximum power is increased in the field weakening region. The characteristic current is shifted to left side by two-conditions. First condition is the increase of no-load linkage flux by more usage of PM. However the usage of PM is limited in IPMSM due to some problems. Second condition is the decrease of d-axis inductance by increase of d-axis reluctance. This is useful for improving maximum power by simple redesigning rotor ribs.

In this paper, the method improving the maximum power without more usage of permanent magnet is suggested. The suggested method is the shifted of the characteristic current through the rib redesign of IPMSM. The detailed analysis results of using the finite element analysis (FEA) and equivalent circuit analysis (ECA) will be presented.

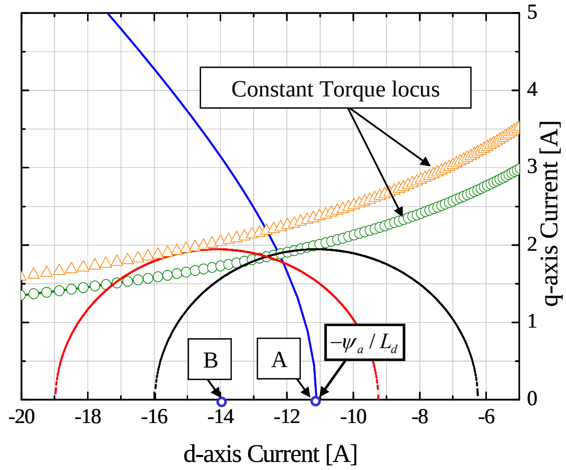

Fig. 2. Voltage ellipses and constant torque locus

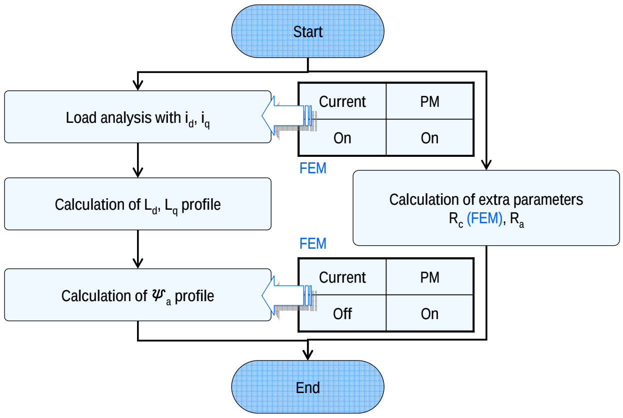

Fig. 3. Overall Process of equivalent circuit analysis (ECA)

IV. Calculation of Parameters in IPMSM

A. Overall Process of Equivalent Circuit Analysis (ECA)

Overall process of equivalent circuit analysis (ECA) is shown in Fig. 3. The difference according to current intensity is considered calculating the flux linkage. Profile of *d, q*-axis inductance and current, current phase angle are calculated to consider nonlinearity [4]. The *d, q*-axis inductance can be computed by relation between intensity of flux linkage and status under no-loaded and loaded condition through equation (6).

$$L_d = \frac{\psi_a - \psi_o \cos\alpha}{i_d}, \quad L_q = \frac{\psi_o \sin\alpha}{i_q} \quad (6)$$

B. Different Rib Thickness of Two IPMSM Model

Two IPMSM models which have different rib thickness are shown by Fig. 4. IPMSM model which has a specification as TABLE I is shown by first figure. The model which has reduced rib thickness by redesigning is shown by second figure. The maximum output which increased in weakening region can be confirmed and the characteristic of IPMSM which is changing can be observed by FEA and ECA reducing rib thickness.

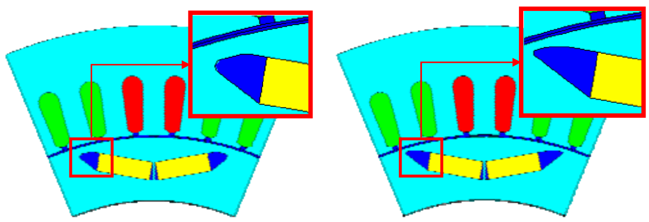

(a) base model (b) rib-redesign model

Fig. 4. Different Rib Thickness of Two IPMSM Model

TABLE I
SPECIFICATION OF BASE MODEL

Specification	Values	Note
Number of pole and slots	8 / 48	-
Winding method	Distributed winding	Short pitch (5/6)
DC link voltage	208 V_{DC}	-
Input current	245 Arms	-
Max speed	8000 rpm	-
Max power	49.3 kW	-

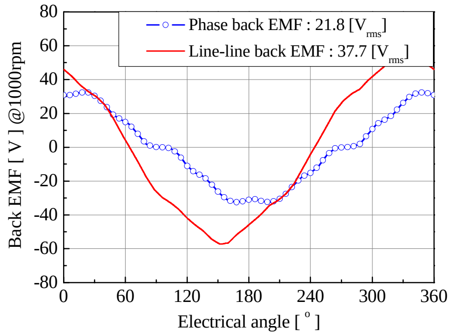

(a) base model

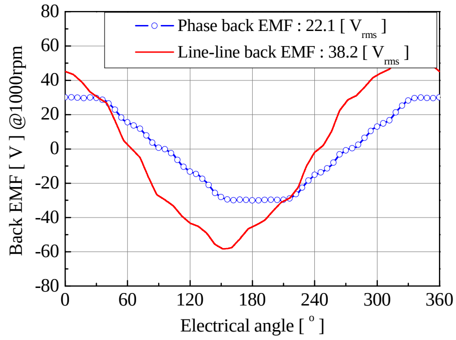

(b) rib-redesign model

Fig. 5. The Back EMF of Two IPMSM

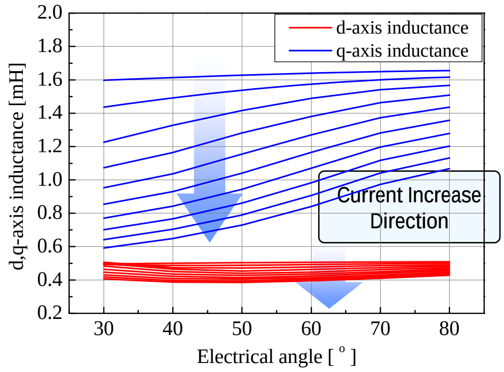

(a) base model

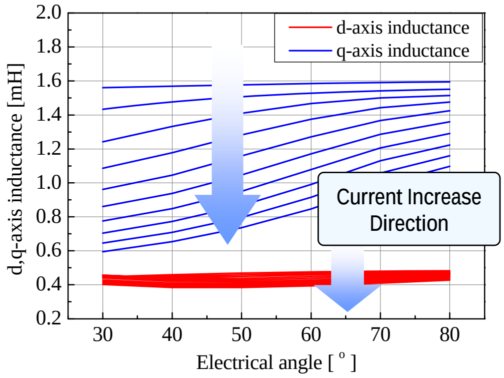

(b) rib-redesign model

Fig. 6. *d, q*-axis inductance of Two IPMSM

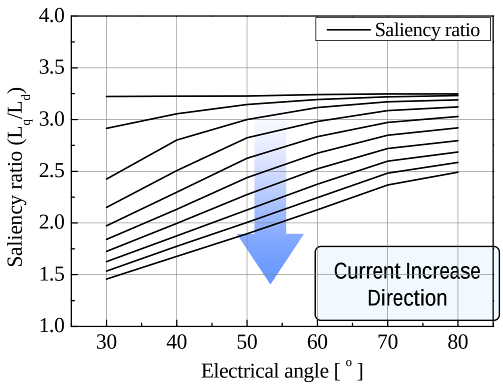

(a) base model

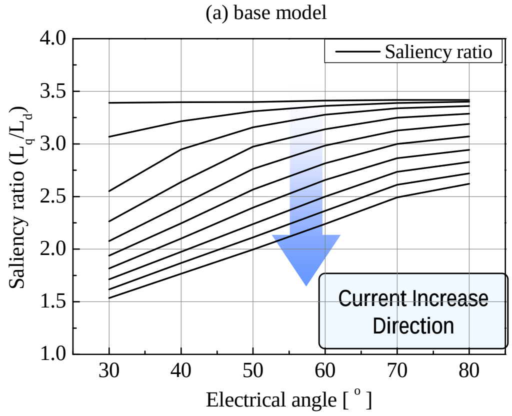

(b) rib-redesign model

Fig. 7. Saliency ratio of Two IPMSM

C. *Calculation of Parameters in IPMSM*

The characteristic current which is moved by redesigning rib lastly can be confirmed. The back EMF which is calculated by flux linkage under no-load condition is shown by Fig. 5. 1.3 percentage of increase in back EMF can be known by reduction of magnetic flux leakage decreasing rib thickness.

The *d, q*-axis inductance and saliency ratio are shown by Fig. 6. and Fig. 7. *Q*-axis inductance increased in small quantity, but *d*-axis inductance decreased by 8 percent. The Components of reluctance torque increase as saliency ratio which is calculated by the ratio of *q*-axis inductance and *d*-axis inductance. The larger maximum power can be obtained by reducing rib thickness eventually.

V. RESULT

Parameters of two IPMSM which have different rib thickness are confirmed by FEA and ECA. *D*-axis inductance which is one of the IPMSM parameter is most influenced by reduction of rib thickness therefore it decreases sharply.

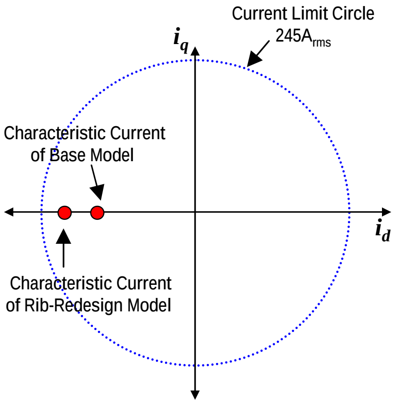

Fig. 8. Shift of the characteristic current within the current limit circle

TABLE Ⅱ
COMPARED OF THE PARAMETERS OF TWO IPMSM

Parameter	Base Model	Rib-Redesign Model
Flux Linkage	0.09 Wb (0%)	0.092 Wb (2%)
Q-axis Inductance	0.453 mH (0%)	0.424 mH (-6.4%)
Characteristic Current	198.7 Arms (0%)	217 Arms (9.2%)
Max power	49.3 kW (0%)	52.3 kW (6.2%)

Characteristic current moves to the left with same size of voltage ellipse. As a result maximum power increases owing to the intersection of the voltage ellipse and constant torque locus. Flux linkage, *d*-axis inductance and characteristic current calculated by FEA and ECA are shown by TABLE Ⅱ. The result that increased characteristic current moved to the left can be known within the current limit circle by Fig. 8.

VI. CONCLUSION

In this paper, the method improving the maximum power without more usage of permanent magnet is suggested. The suggested method is the shifted of the characteristic current through the rib redesign of IPMSM. As the rib is redesigned, *d*-axis inductance is largely decreased. The analysis results of using the FEA and ECA is shown. As a result, by redesigning the rotor rib, maximum power increased by 6.2%. Due to reduction of rib thickness, the stress concentration can increase at the rotor rib. Therefore structure analysis is sometimes demanded.

VII. REFERENCES

[1] J.-W. Jung, J.-J. Lee, S.-O. Kwon, and J.-P. Hong, "Equivalent Circuit Analysis of Interior Permanent Magnet Synchronous Motor Considering Magnetic Saturation," *Electric Vehicle Symposium 24 (EVS)*, May. 2009

[2] Dutta. R, Rahman. M. F, "Investigation of Suitable Vector Control Techiques for Low Voltage IPM Machine in 42V System," *in Proc. IEEE. Ind. Elec. Soc. 30th Annu. Conf. Paper*., Vol. 3, pp. 2724 – 2728, November. 2004

[3] Z. X. Fu, "Pseudo Constant Power Times Speed Operation In The Field Weakening Region of IPM Synchronous Machines," *in Proc. IAS. Ind. Appl. 38th Annu. Conf. paper.,* Vol. 1, pp. 373-379, October. 2003.